

# DYNAMICS AND CLEARANCE ANALYSIS OF NASA'S SPACE LAUNCH SYSTEM BLOCK-1 AND BLOCK-1B SOLID ROCKET BOOSTER SEPARATION EVENT

**Carole J. Addona<sup>\*</sup>, Michael M. Sanders<sup>†</sup>, Benjamin S. Burger<sup>‡</sup>, William J. Harlin<sup>§</sup>, Rekesh M. Ali<sup>\*\*</sup>, Zachary T. Muscha<sup>††</sup>, Peter J. McDonough<sup>‡‡</sup>, Jared T. Rucker<sup>§§</sup>, Drake A. Ranquist<sup>\*\*\*</sup>**

NASA's Space Launch System (SLS) solid rocket booster separation event is an essential area of study requiring high fidelity modelling to capture the complexity of an intra-atmospheric stage separation event. The setup and analysis for this event leveraged the NASA-developed CLVTOPS multi-body dynamics toolchain to model aerodynamics at the separation event, booster thrust tailoff, and Core Stage engine throttling in addition to the separation system itself (booster separation motors (BSMs), pyrotechnic bolts and struts). The approach documented here will give a brief background on the CLVTOPS toolchain, how key input models are integrated and verified, and how results are quantified using an ordered-statistics approach. Specific areas discussed herein address the performance-to-orbit realized by adjusting the delay time between the separation cue and the actual separation event, and how the orientation of the aft BSMs was tuned to address small clearances between the aft diagonal attach struts and the Core Stage. Post-flight results from the inaugural Artemis I flight are also shown, and validation is performed between predicted vs. actual separation dynamics and clearances. Challenging night launch conditions necessitated comparisons that were more qualitative in nature, but still showed very good agreement to pre-flight predictions.

---

<sup>\*</sup> SLS Liftoff and Separation Dynamics Technical Lead, EV42 Guidance, Navigation, and Mission Analysis Branch, Amentum Space Exploration Division (ASED)/Amentum, Huntsville, AL 35806

<sup>†</sup> Aerospace Engineer, EV42 Guidance, Navigation, and Mission Analysis Branch, ASED/Amentum, Huntsville, AL 35806

<sup>‡</sup> SLS Flight Mechanics Co-Lead, EV42 Guidance, Navigation, and Mission Analysis Branch, NASA/MSFC, Huntsville, AL 35812

<sup>§</sup> SLS Flight Mechanics Co-Lead, EV42 Guidance, Navigation, and Mission Analysis Branch, ASED/McLaurin Aerospace, Knoxville, TN 37929

<sup>\*\*</sup> Aerospace Engineer, EV42 Guidance, Navigation, and Mission Analysis Branch, ASED/McLaurin Aerospace, Knoxville, TN 37929

<sup>††</sup> Aerospace Engineer, EV42 Guidance, Navigation, and Mission Analysis Branch, ASED/Amentum, Huntsville, AL 35806

<sup>‡‡</sup> EV42 ESSCA Lead; EV42 Guidance, Navigation, and Mission Analysis Branch, ASED/Amentum, Huntsville, AL 35806

<sup>§§</sup> Aerospace Engineer, EV42 Guidance, Navigation, and Mission Analysis Branch, ASED/Amentum, Huntsville, AL 35806

<sup>\*\*\*</sup> Aerospace Engineer, EV42 Guidance, Navigation, and Mission Analysis Branch, ASED/Amentum, Huntsville, AL 35806

## INTRODUCTION

The launch of Apollo 11 on July 16, 1969, and the subsequent first steps on the moon on July 20, marked the opening of an era. Apollo 17, launched only 3 short years later, left the moon on December 14, 1972, marking the last time any human set foot on the surface of the moon<sup>1</sup>. Fast forward 45 years, and with the signing of Space Policy Directive-1 on December 11, 2017\*, the Artemis program was born.

Artemis is the first National Aeronautics and Space Administration (NASA) program since Apollo whose purpose is returning mankind to the moon, and eventually to Mars. The Space Launch System (SLS) is the vehicle designed and built to provide the heavy launch capability it will take to return humans to the moon, plus provide heavy-lift payload capability for several components of the planned Gateway lunar orbital space station<sup>†‡</sup>.

SLS takes advantage of several design features of its NASA predecessors. Like the Saturn V, SLS is a multi-stage-to-orbit rocket; like the Space Shuttle, SLS inherits the use of two disposable solid rocket boosters (SRBs), which provide more than 75% of the total vehicle thrust at launch<sup>§</sup>. There are currently three planned variants of the SLS vehicle: Block 1 (Artemis missions I-III), Block 1B (Artemis missions IV-IIIIV), and Block 2 (Artemis IX+ missions). See Figure 1 for a graphic depicting each variant.

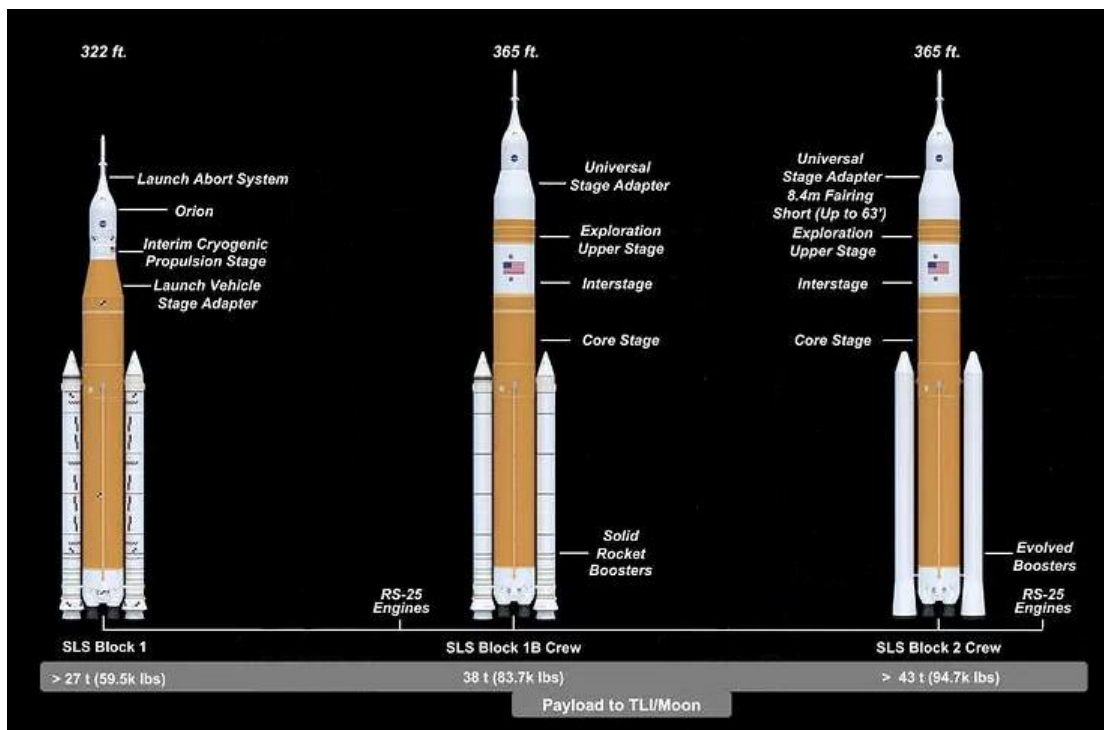


**Figure 1. SLS Vehicle Configurations\*\*.** Note the increased payload to translunar injection (TLI) expected with each subsequent vehicle configuration.

\* <https://trumpwhitehouse.archives.gov/presidential-actions/presidential-memorandum-reinvigorating-americas-human-space-exploration-program/>

† <https://www.nasa.gov/humans-in-space/artemis/>

‡ <https://www.nasa.gov/mission/gateway/>

§ [https://www.nasa.gov/wp-content/uploads/2017/05/8690sls\\_solid\\_rocket\\_booster\\_fact\\_sheetfinal083072015\\_508.pdf](https://www.nasa.gov/wp-content/uploads/2017/05/8690sls_solid_rocket_booster_fact_sheetfinal083072015_508.pdf)

\*\* <https://www.nasa.gov/image-article/sls-block-1-crew-block-1b-crew-block-1b-cargo-block-2-cargo-evolution/>

While the booster separation event represents only a small fraction of the total mission timeline, its complex and dynamic nature warrants thorough analysis to provide confidence that the booster separation event will be successful. This paper will address modeling and simulation of the SLS booster separation event by:

- providing an overview of a notional booster separation event timeline;
- discussing the simulation toolchain used to integrate these models and produce quantified statistical results;
- describing input models that are primary drivers of booster separation performance;
- presenting key areas of analysis performed to assess separation clearance;
- comparing pre-flight predictions to flight data from Artemis I, launched on November 16, 2022.

## **BOOSTER SEPARATION EVENT OVERVIEW**

The SLS booster separation sequence nominally begins when the mid-value of three pressure transducers mounted in the head-end of either booster falls below a threshold value, the same approach that was utilized for Space Shuttle SRB separation<sup>3,4</sup>. For SLS SRB separation, when the first SRB reaches this threshold pressure, the four Core Stage RS-25 engines (CSEs) begin throttling down to limit the tension load experienced by the attach bolts connecting each SRB to the Core Stage. This tension load is a result of the Core Stage starting to “drag” the spent boosters along.

Once both SRBs reach the pressure threshold, the booster separation sequence is initiated. A pre-determined separation delay follows (variable, based on mission requirements), during which the SRB nozzles are moved to their “null” position, all the separation pyrotechnic devices are armed, and the SRB thrust decays further. Once the separation delay has elapsed, several events happen nearly simultaneously:

- The SLS Guidance Flight Software (FSW) commands an attitude hold to prevent the vehicle from inadvertently steering in a way that reduces separation clearances.
- Frangible bolts are severed in each of the four attaches connecting the SRBs to the Core Stage (one bolt at the forward attach ball/socket joint, three bolts inside the aft struts, for each SRB).
- 16 booster separation motors (BSMs) are fired (oriented four to a cluster on the forward and aft ends of each booster).

The BSMs radially accelerate the boosters away from the vehicle, and the Core Stage engines begin throttling back up to their full rated power level. After separation, the commanded attitude hold ends and the Core Stage proceeds to its target orbital insertion point, and the SRBs splashdown in the Atlantic Ocean about six minutes after launch. Unlike the Shuttle program, the SRBs used for SLS are not being recovered. Reference Table 1 for a consolidated timeline of the events described above.

**Table 1. Notional Booster Separation Event Timeline.**

Event	Time (sec)*
Separation logic activated	Launch + 110
RS-25s throttle down	Variable time after 110
Both boosters reach appropriate chamber pressure	Separation Cue + 0
SRB nozzles move to null position	Separation Cue + 2
Separation command issued	Separation Cue + 9 Separation Time + 0
RS-25s throttle back up to full rated power level	Separation Time + 0
Fire command sent to 16 BSMs and 8 separation bolts	Separation Time + 0
3-Axis attitude hold commanded	Separation Time + 0
Attitude hold disabled/Simulation end time	Separation Time + 5

## SIMULATION ARCHITECTURE OVERVIEW

NASA's Marshall Space Flight Center (MSFC) Liftoff and Separation Dynamics team uses the CLVTOPS<sup>2</sup> multi-body dynamics simulation to perform separation analyses. CLVTOPS is a wrapper around TREETOPS<sup>†</sup> (which is a generic time history simulation tool originally developed under NASA funding to analyze complex multi-body flexible structures with active control elements) and provides the ability to add launch vehicle-specific inputs as well as the capability to run Monte Carlo simulations. Once simulations are complete, post-processing is handled in CLVTOPS using a variety of custom scripts and the NASA-developed TREE3D<sup>‡</sup> visualization tool that take advantage of the functionality offered by Python<sup>§</sup>, MATLAB<sup>\*\*</sup>, gnuplot<sup>††</sup>, and Visualization Toolkit (VTK)<sup>3</sup> to reformat and optimize CLVTOPS output into forms easily digestible by analysts, engineers, and senior management. The composite of the tools in the CLVTOPS toolchain is used to simulate the dynamics of each body that comprises the SLS vehicle during the booster separation event.

---

\* Notional times given. Actual values will differ per vehicle/flight.

<sup>†</sup> <https://software.nasa.gov/software/MFS-33566-1>

<sup>‡</sup> <https://software.nasa.gov/software/MFS-34076-1>

<sup>§</sup> <http://www.python.org>

<sup>\*\*</sup> <http://www.mathworks.com>

<sup>††</sup> <http://www.gnuplot.info>

## KEY INPUT MODELS

The baseline booster separation simulation in CLVTOPS consists of three bodies (one rigid Core vehicle and two flexible SRBs), each with six rigid body degrees-of-freedom (DOF) and multiple modal DOFs. Additionally, there are several ancillary bodies with reduced or no DOFs, used for bookkeeping or for slosh and nozzle dynamics modeling. Some particularly unique aspects of this simulation are that it starts at launch and models the entire ascent trajectory up to and including booster separation, using the actual SLS GN&C FSW and varying mass properties as the vehicle expends propellant. Typically, two separate simulations are used – one to establish the states at separation, and one to do the actual detailed separation analysis starting with those states (this was the case during the Shuttle program<sup>4,5</sup>).

This section will present some of the most influential input models that are incorporated into CLVTOPS for analyzing the booster separation event.

**Body Attach Modeling.** The SLS design utilizes four structural attach points (Figure 2) to connect each SRB to the Core Stage, in the same manner as the Space Shuttle's SRBs were connected to the External Tank (ET). Near the forward end of each booster is a single forward attach point – consisting of a ball and socket fitting held in place by a frangible bolt – which is the primary load path for the axial loads generated by the SRB. Additionally on the aft end, each SRB has three struts (upper, diagonal, lower) which assist the forward attaches in holding the SRB to the Core Stage by restricting lateral and rotational motion between the stages. Each strut is composed of two halves (or stubs) that are held together by a frangible bolt. At the time of separation, commands are sent to detonate the pyrotechnics of the frangible bolts in the attaches and the SRBs are released.

In the CLVTOPS booster separation simulation, the four structural interfaces for each booster are modeled with four linear spring/damper devices. The stiffness and damping values assigned were chosen such that they allow very little pre-separation relative motion between the Core Stage and SRBs while still maintaining numerical stability. These values are set to zero at separation, releasing the SRBs from the rest of the vehicle. These stiffness and damping values are somewhat arbitrary for the purposes of simulation, and do not necessarily represent actual structural hardware numbers. Sensitivity studies were conducted to verify the implementation of this modeling methodology; rigid body sensitivity to attach stiffness was assessed by running Monte Carlo simulations

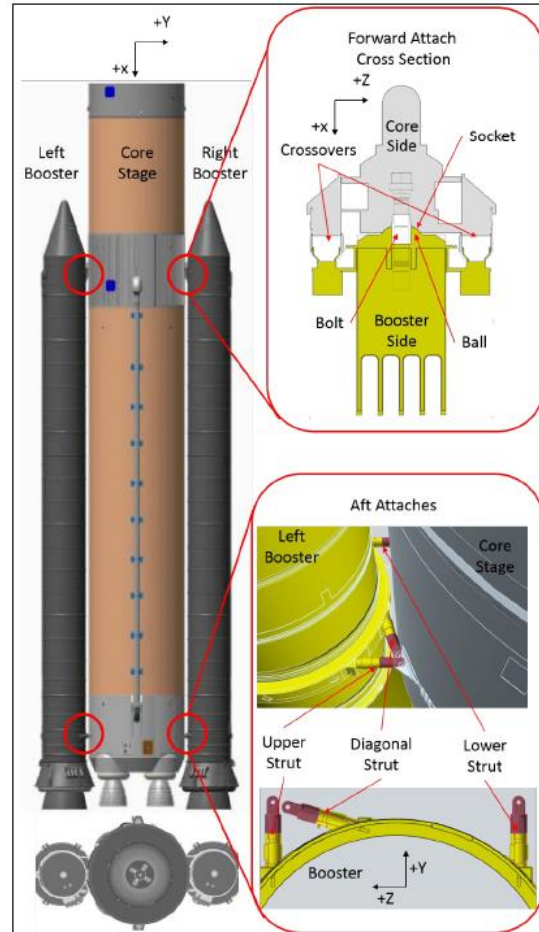


**Figure 2. SRB-Core Stage Attach Locations.** Each connection point is modeled as a linear spring-damper with high stiffness/damping values to limit motion prior to separation.

with the stiffness values increased and decreased by an order of magnitude. Negligible differences in clearance results were found.

**Booster Separation Motor (BSM) Model.** There are eight BSMs per SRB, situated four to a cluster in the forward frustum and on the aft skirt of each SRB (Figure 3). The BSMs provide the force needed to accelerate the SRBs radially away from the Core Stage during separation. SLS utilizes the same BSM design and separation scheme as the Shuttle program; at separation the SRBs are propelled “up” (away from Earth) and “out” (radially to the trajectory) from the Core Stage. This separation trajectory was chosen to avoid any interference with Shuttle Orbiter wings; SLS does not have this same hardware restriction, but takes advantage of the heritage configuration.

BSMs are modeled in CLVTOPS using a vendor-provided FORTRAN-based model, which generates 16 individual thrust profiles based on heritage BSM test data and two user-provided inputs: temperature (BSM Propellant Mean Bulk Temperature, or PMBT), and a single dispersion parameter (per BSM) meant to capture dispersions in ignition interval, pressure rise rate, and maximum pressure. Verification was performed by comparing CLVTOPS BSM output to vendor-provided unit tests.

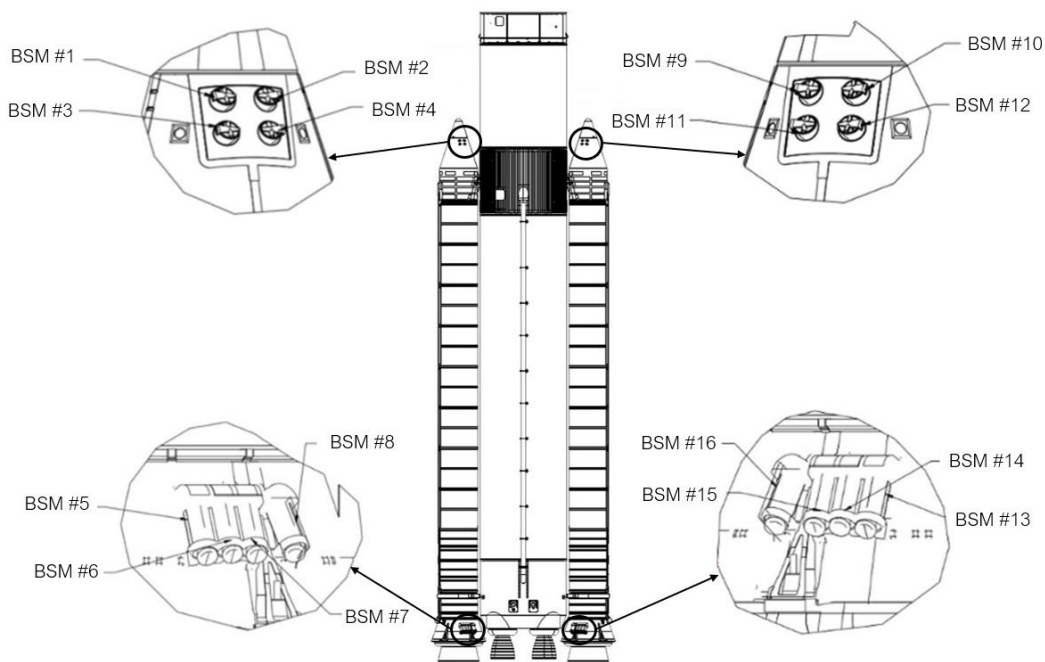


**Figure 3. SLS Booster Separation Motor Locations.** Four BSMs each on the nose cone and aft skirt of each SRB provide the needed radial acceleration to generate clearance.

**Booster Separation Aerodynamics.** One of the most complex and influential input models for the booster separation event is the separation aerodynamics model<sup>6</sup>. Multiple factors result in a complicated environment in which to determine aerodynamics and plume impingement (from both the BSMs and the Core Stage RS-25s) forces and moments on the vehicle, such as SRBs translating and rotating relative to the Core vehicle, Core engines throttling and gimbaling, SRBs rapidly tailing off, and changing altitude, Mach number, and dynamic pressure. After physical separation (connections have been severed, BSMs have completed firing), the only outside influence on the SRBs is the atmospheric environment and plume impingement effects from the Core Stage RS-25s. The separation aerodynamics model consists of a table of coefficients generated for each body (Core and right and left SRBs) using 11 independent inputs: x, y, and z locations; roll, pitch, and

yaw rotations; angles of attack and sideslip, dynamic pressure, Mach number, and BSM thrust. At each simulation timestep, CLVTOPS queries the database with these trajectory inputs, and the resulting coefficients are processed into forces and moments that are applied to each of the three bodies (Core, left SRB, right SRB). An idea of the magnitude of the effect of this model on booster trajectories can be seen in Figure 4. The inclusion of aerodynamic effects significantly increases the variation in SRB paths post-separation, which affects various Core-to-SRB clearances.

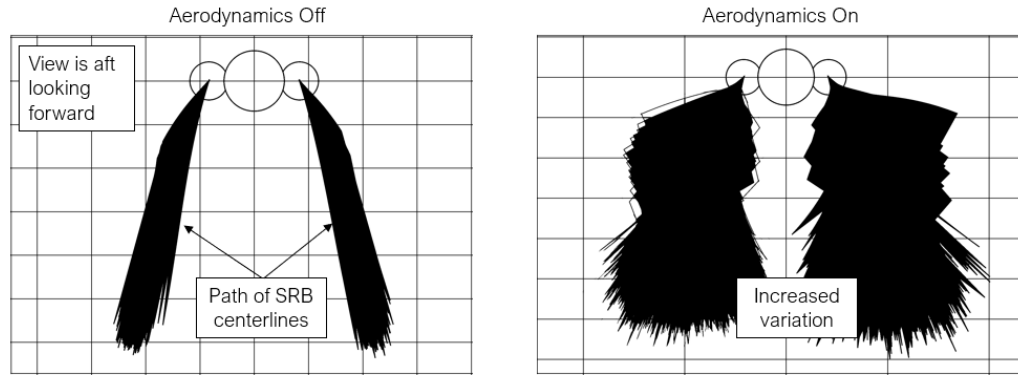


**Figure 4. Comparison of Aerodynamic Model On vs. Off.** *The inclusion of aerodynamic effects greatly influences the SRB path post-separation and is a key driver of any SRB-SRB predicted contact after separation from the Core Stage.*

**Booster Separation Logic.** The SLS booster separation logic is modeled after the Space Shuttle’s SRB separation logic, and contains several features developed during the Shuttle program to handle anomalies and ensure safe separation. These features are implemented in CLVTOPS, which replicates as closely as possible the actual FSW logic flow.

- Flight software does not start monitoring for booster separation conditions (i.e., chamber pressure) before a pre-determined-per-flight Mission Elapsed Time (MET). This ensures that the separation event does not start prematurely.
- There is a pre-determined-per-flight MET time that the separation sequence will start (a “backup timer”) if it has not already been initiated before this time. This ensures that the booster separation event will not start too late.
- Based on historical SRB thrust data from Shuttle flights and SRB test motor firing, there is a set time between when both boosters are expected to reach the threshold pressure cue. If this time is violated, separation is begun at the backup timer MET. This ensures that if there are higher-than-expected differences in SRB tailoff thrust, separation will still proceed at an appropriate MET time.
- Once the separation sequence has been triggered, there is a set delay time (measured in seconds) before the SRBs physically separate from the Core vehicle. This time allows the separation pyrotechnic systems to be armed, the SRB nozzles to move to the null position, and allows the SRB thrust to tailoff further.

CLVTOPS implements this separation logic through its Mission Manager capability, and resulting sequences of events and event times undergo a comprehensive peer review with other independent 6-DOF SLS simulations (Marshall Aerospace Vehicle Representation in C (MAVERIC<sup>7</sup>),



and Program to Optimize Simulation Trajectories 2 (POST2<sup>\*</sup>)), providing confidence that the logic has been implemented correctly.

**Clearance Models.** To determine separation clearances, after CLVTOPS has completed each simulation, the resultant trajectories are combined with 3D models of the actual SLS hardware and assessed through time for any contact/recontact as well as the closest distance between pairs of 3D models. Currently, SLS booster separation analysis performs 33 different clearance computations using 26 different 3D models. Each 3D model is derived from a nominal/static Computer Aided Design (CAD) model and converted to a polygon-based 3D mesh. Because initial clearances are so small in most areas, great care was taken to generate high-polygon count meshes for each model, giving an acceptable level of resolution from which to assess clearance. Figure 5 illustrates a visual depiction of each clearance pair, using the TREE3D modeling tool. TREE3D was developed specifically to ingest CLVTOPS-generated trajectory output; a feature shown in Figure 5 is the ability to visually represent the closest distance between each clearance pair by a line. The distances represented at each simulation timestep are output to a datafile for detailed analysis.

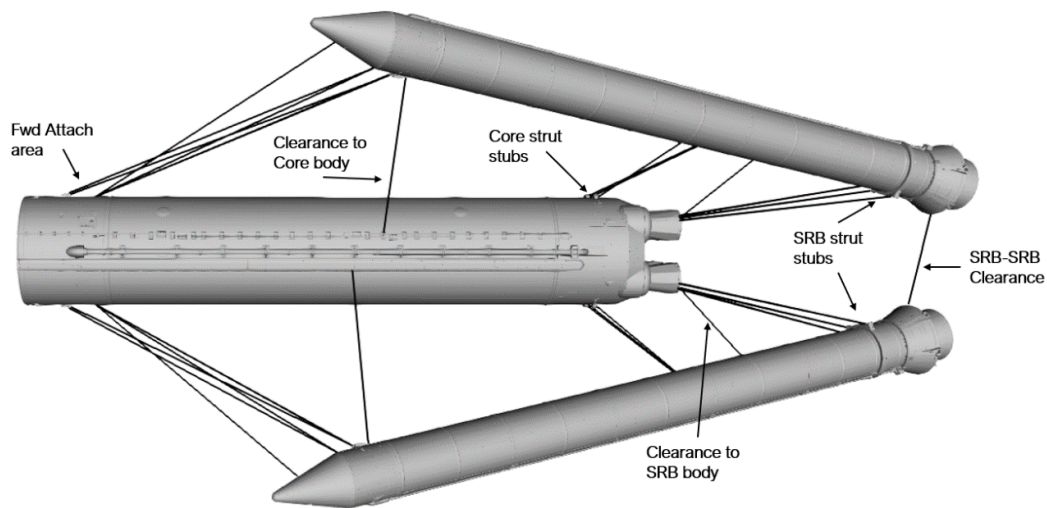


**Figure 5. Example of Minimum Distance Tool distance calculation.** *Each line represents one of the 33 clearance pairs. TREE3D allows easy visualization of any areas of concern.*

**Booster Thrust Model.** Like the BSM implementation, SRB thrust from liftoff through the separation event is modeled using a vendor-provided FORTRAN module that generates steady state and tailoff ballistic performance of the SRB motor. The provided model produces variation from the nominal thrust trace by dispersing various inputs such as nozzle erosion, motor efficiency, grain geometry, PMBT, burn rate, etc. The model also tracks parameters relevant to the booster state based on the simulated performance, such as booster mass, remaining propellant, internal pressure, and thrust imbalance between the pair of SRBs. Implementation and verification of the model was relatively straightforward, since the code was contained in a stand-alone FORTRAN module that could be “dropped in” with the existing source code. Comparisons with vendor-provided unit tests served to verify the integration of the module, and comparisons with other independent 6-DOF SLS trajectory simulations provided confidence that it was implemented correctly into the overall integrated vehicle simulation.

---

<sup>\*</sup> <https://post2.larc.nasa.gov>



## RESULTS QUANTIFICATION

The SLS program requires all separation event analyses to show a 99.865% probability with 90% confidence of a successful booster-Core Stage separation during nominal operation, and 99.725% success rate with 90% confidence for failure scenarios (for booster separation, a failure scenario would be one Core Stage engine out or one random BSM out on either booster per run). These metrics are also called “ $3\sigma$  low,” and “ $2\sigma$  low,” respectively, referring to the low end of the clearance value distributions and their distance from the mean clearance. Simulations for SLS missions use a Monte Carlo approach, which involves dispersing model input values along a distribution and running hundreds or thousands of variants of the simulation. The “ $3\sigma$  low” metric corresponds to zero observed failures out of 2000 Monte Carlo simulations, while the “ $2\sigma$  low” metric allows for 36 failures out of 2000 runs. All the  $3\sigma$  or  $2\sigma$  metrics are calculated using “ordered statistics”, the details of which can be found in Hanson and Beard<sup>8</sup>. In summary, each set of 2000 output values is placed in numerical order, and the  $3\sigma$  statistic is the result of interpolating the 1999<sup>th</sup> and 2000<sup>th</sup> run (for  $3\sigma$  high), or interpolating between the 1<sup>st</sup> and 2<sup>nd</sup> runs (for  $3\sigma$  low), depending on how the data is sorted (ascending or descending order).

The benefit of taking a Monte Carlo approach instead of other methods (worst-on-worst, root-sum-square or variations, etc.) is that the Monte Carlo approach makes fewer assumptions about the relationships between the input models; for instance, worst-on-worst analysis assumes that the worst vehicle behavior is caused by extreme values in all inputs, which is not necessarily the case. By using random variations in inputs and sufficiently sampling the probability space, it is possible to quantify the success rate and confidence level of the system design without making erroneous assumptions related to the input terms.

## BOOSTER SEPARATION ANALYSIS RESULTS

Now that a discussion of the CLVTOPS booster separation simulation and results quantification has been completed, the following sections will present how to recognize analysis trends relevant to booster separation, as well as two case studies of how these trends were used to increase vehicle performance or clearance.

### Analysis Trends

There are two significant areas of observation used to assess analysis results for the booster separation event: 1) how clearances increase, maintain, or decrease after initial separation, and 2) how these clearances change (or not) when compared over many different simulations over time.

*Increasing Clearance Example.* If a given clearance pair’s relative distance is always increasing, and this trend holds over time when different vehicle configurations are assessed, this is a good indication that there is a low sensitivity to input model changes or conditions at separation. An example of such a clearance pair is the Core-side aft upper strut stub-to-SRB clearance (Figure 6). The top pair of figures show the orientation of one SRB to the Core in the mated configuration and a few moments post-separation. Due to the separation design, the SRB will always move away from the core-side-upper-strut-stub, therefore clearance is always expected to increase. This is exhibited in the time-history plot in Figure 6. This is an example of clearance that increases after separation without any ‘dips’ (which would indicate the Core and SRB are moving back towards each other), and these trends have been relatively unchanged since early SLS booster separation analyses. This trend would not be expected to change, simply due to the hardware configuration.

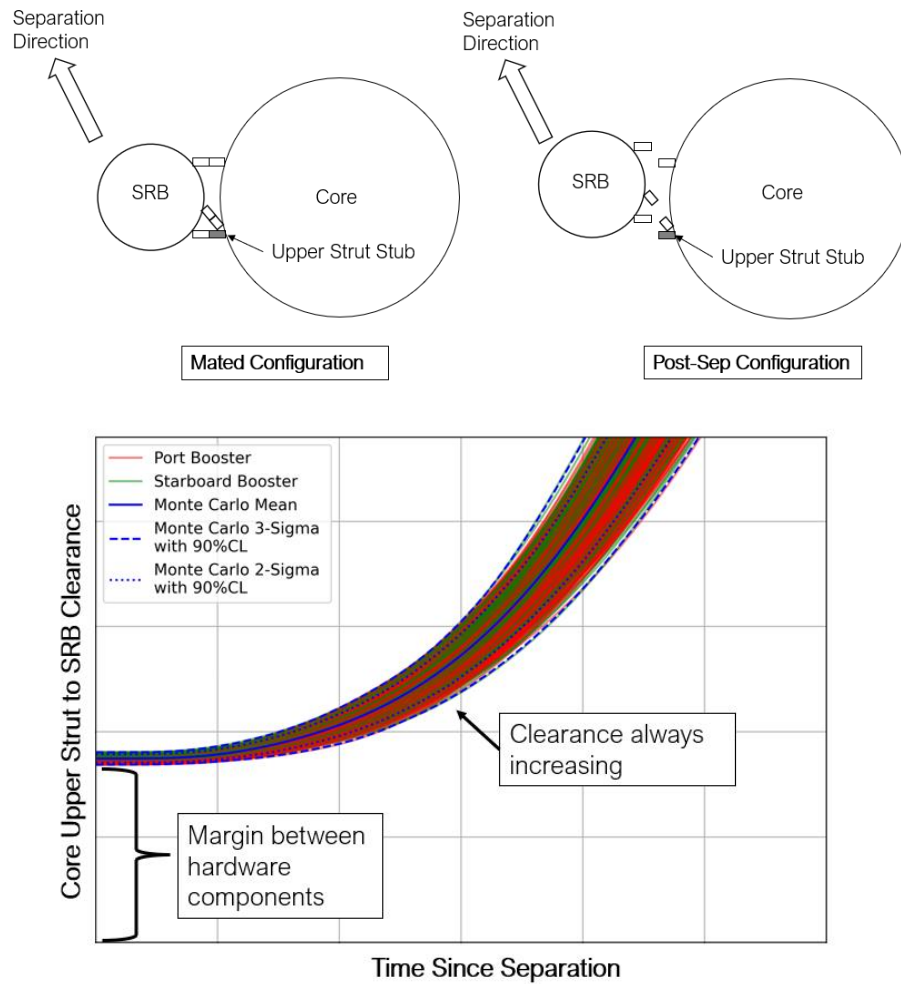


**Figure 6. Core Upper Strut Stub to SRB Clearance.** *Note that this particular clearance pair is between the Core strut stub and the SRB body, thus the non-zero starting clearance.*

*Variable Clearance Example.* Figure 7 is representative of a clearance pair that exhibits decreasing-then-increasing clearance. The ‘dips’ indicate that the lower strut stub is temporarily approaching the SRB body, but adequate hardware margin is still maintained, and this trend has been consistent over several years of analysis. This is a clearance pair that might show more sensitivity to model updates or states at separation than the previous pair; whereas the hardware design assures that the upper strut will always show good clearance, since the lower strut is in the direction of separation, changes in forcing functions such as aerodynamic forces and BSM thrust vector etc. might have a noticeable effect on lower strut clearance.

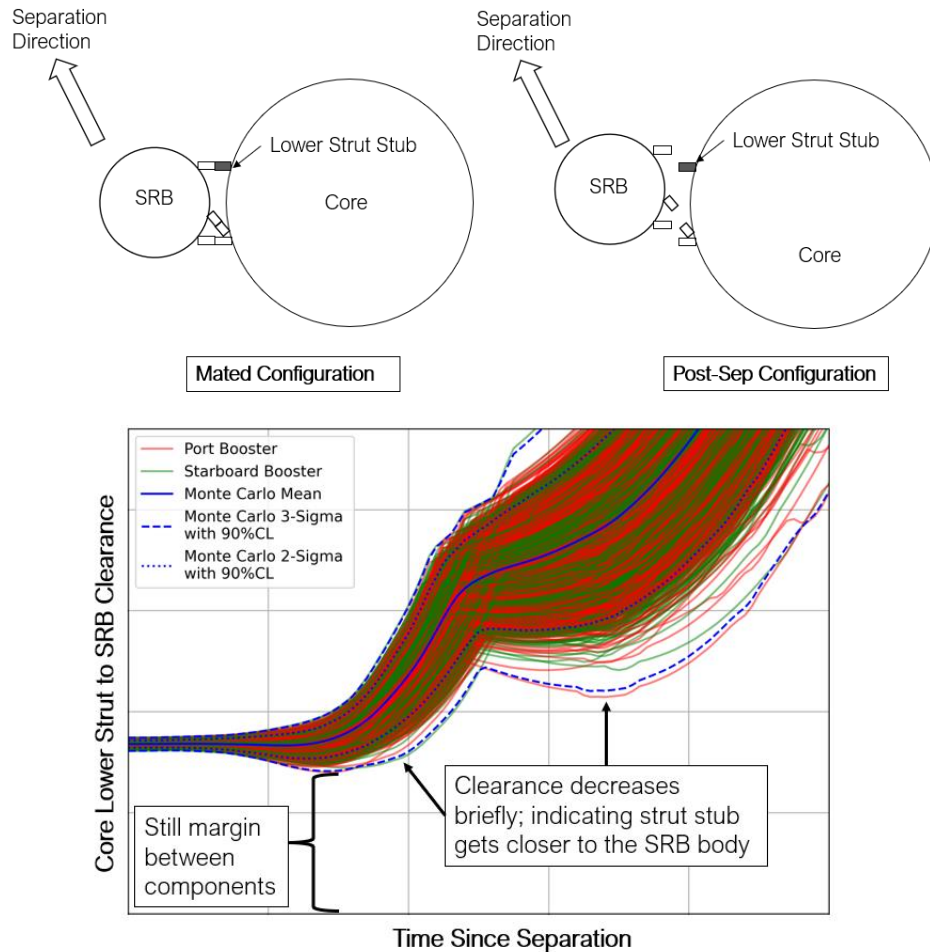


**Figure 7. Core Lower Strut to SRB Clearance.** *The Core lower strut stub briefly gets closer to the SRB body during separation, temporarily decreasing clearance.*

## Case Studies

During each booster separation analysis cycle, several different vehicle configurations and model input variations are studied, using the Monte Carlo methodology. Results from these Monte Carlo cases are used to inform configuration or design changes that are desired to enhance the particular Artemis mission. The following two case studies will discuss changes incorporated to increase the robustness of the aft diagonal strut clearance, and a timing change to realize more mass-to-orbit.

*Case Study 1: Increasing Aft Diagonal Strut Clearance.* SLS booster separation analysis results showed very tight clearance, and sometimes contacts (only for stressing vehicle configurations or failure scenarios) of the SRB-side diagonal strut stub to the Core Stage. SLS inherited the separation design used on Shuttle, and this heritage configuration resulted in a roll of the booster during separation due to the offset line of action of the aft BSM cluster relative to the SRB centerline (Figure 8). This roll motion rotated the SRB-side diagonal strut stub towards the Core Stage engine section, causing low clearance margins and/or contact probability. This was not a concern for Shuttle because the aft struts were mounted to the aft-most portion of the External Tank (ET), at the transition between the tank cylinder and the aft dome, leaving nothing for the booster struts to contact after separation. Conversely, the SLS Core Stage has tens of feet of cylindrical engine section below the aft strut mounts (Figure 9).

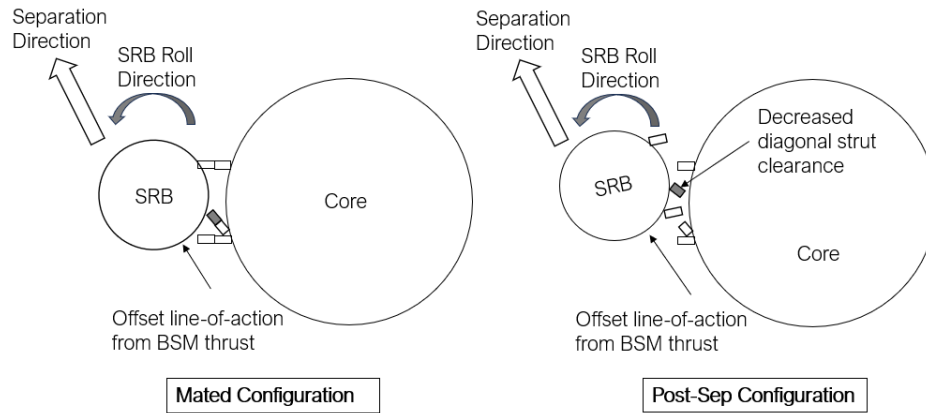


**Figure 8. Illustration of Roll Induced by Offset BSM line-of-action at Separation.** *The heritage design resulted in reduced SLS diagonal strut clearance due to the induced roll rate.*

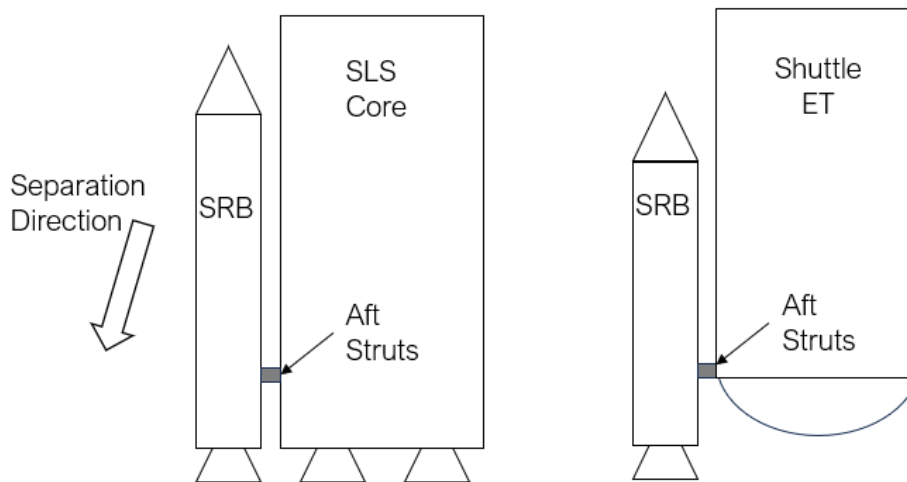


**Figure 9. SLS vs. Shuttle Aft Strut Mounting Locations.** *SLS aft struts must clear tens of feet of Core engine section, whereas on Shuttle the strut stubs immediately had better clearance due to their proximity to the aft dome curvature.*

No issues with the diagonal strut clearance were identified during the Artemis I test flight, but to ensure this clearance was more robust for Artemis II and beyond flights, the aft BSM line-of-action was altered to be on the other side of the SRB centerline (Figure 10). This change induces a roll rate in the opposite direction, which rotates the booster diagonal struts away from the Core Stage during separation and improves diagonal strut clearances with little consequence to other booster-to-Core clearances and overall booster separation trajectories. Additionally, this specific design modification was selected due to its minimal impact to booster hardware and certification, as well as minimal changes to Core Stage engine thermal environments; the BSM plumes are very close to the RS-25s, but this line-of-action change did not result in detrimental impact to the RS-25s. Analysis results showed the desired robustness of the aft diagonal strut clearance to model updates and states at separation was achieved. Many different vehicle configurations, separation delays, and aerodynamic models have been assessed, and this clearance is very stable – it is still

one of the smallest clearances, but now shows virtually no variation regardless of vehicle configuration or input model version.

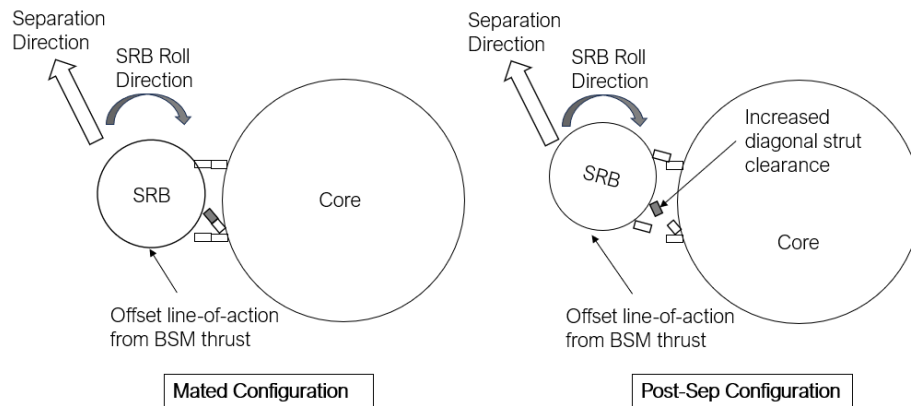


**Figure 10. Illustration of Favorable Roll Induced by Offset BSM line-of-action at Separation.** *The diagonal strut now rotates away from the Core, increasing clearance.*

**Case Study 2: Decreasing Separation Delay to Increase Payload-to-Orbit.** In addition to maintaining clearance between the SRBs and Core during separation, another important consideration is vehicle performance, defined in this context as payload mass-to-orbit. For the inaugural Artemis I flight, it was decided to use a separation delay (time between the separation trigger and physical separation) that was very conservative with regards to clearance. However, this delay came with a mass penalty – each second of delay between the separation trigger and physical separation resulted in a few hundred fewer pounds of payload that could be pushed to orbit. Given that Artemis I was the inaugural test flight and was not performance constrained, a longer, more conservative delay was chosen. This philosophy changed starting with Artemis II – it was desired to reduce the separation delay as much as practicable to maximize vehicle performance (Figure 11).

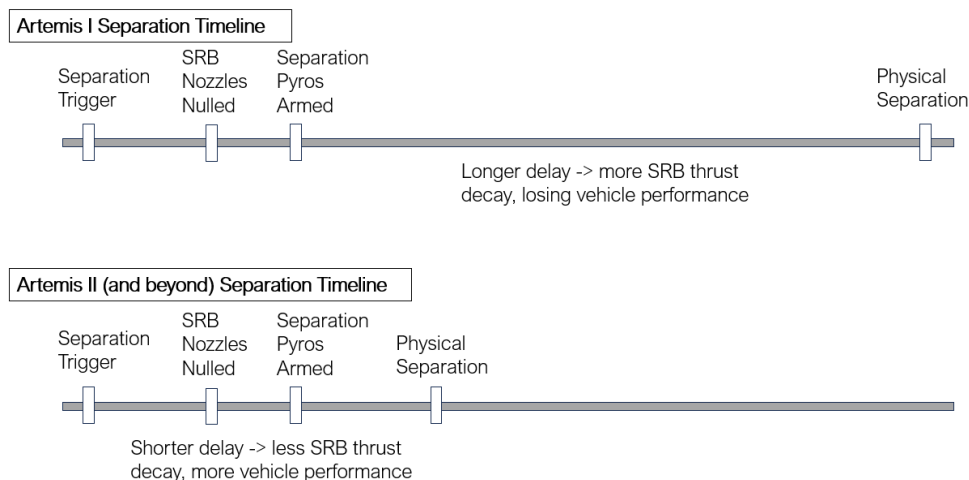


**Figure 11. Artemis I vs. Artemis II (and beyond) Booster Separation Timeline.** *A minimum delay is required for the SRB nozzles to move to the null position and for the separation pyrotechnics to arm. Beyond this, any additional delay is to allow the SRB thrust to continue tailing off, which increases the relative axial acceleration between the SRBs and Core, leading to more conservative separation clearances, but at a cost of payload-mass-to-orbit.*

Analysis results from Artemis I showed the delay could be reduced by several seconds with no issues. When the delay was reduced further, some incidental “rubbing” was observed in the forward attach ball-and-socket joint; the SRB-side ball tended to “slide” out of the Core-side socket instead of “drop” out, leading to this observed rubbing effect. The interface between the SRB-side ball and Core-side socket (reference Figure 12) houses the pyrotechnic bolt that physically connects the forward end of the SRBs and Core together and this joint is designed to transfer the entirety of liftoff/ascent loads generated by the ~7+ million pounds of thrust from the SRBs to the Core Stage. Therefore, this effect would be considered acceptable if 1) the loads stayed within the capability of the hardware and 2) positive clearances were maintained elsewhere when contact dynamics were included in the separation analysis.

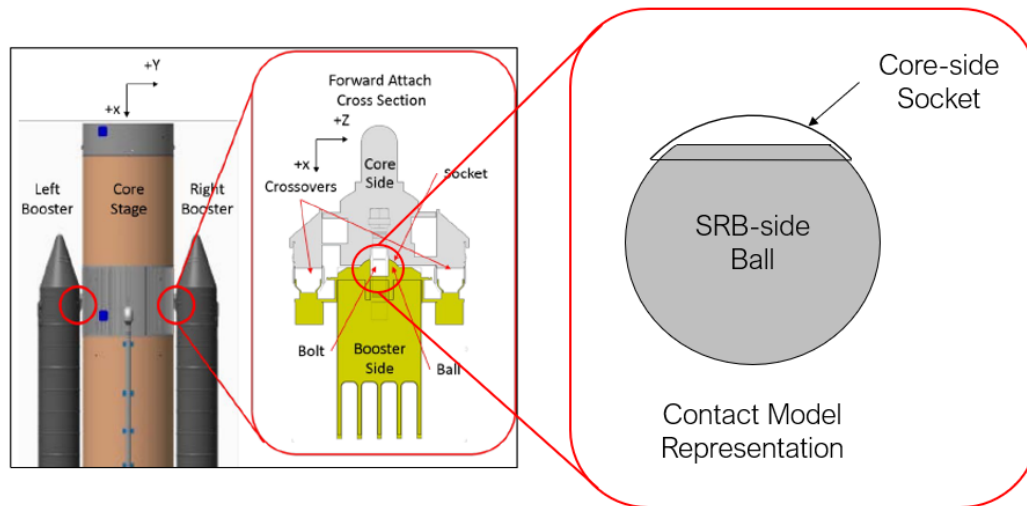


**Figure 12. Ball and Socket Contact Model Parts.** *Ball is modeled as a solid partial sphere; socket is a hollow partial sphere – ball fits inside the socket when in the mated configuration.*

To characterize the nature of this effect, a custom contact model representing the ball and socket hardware was developed in CLVTOPS. A solid partial sphere represents the SRB ball, and a hollow partial sphere represents the Core-side socket (Figure 12). Rubbing is detected when any portion of the ball intersects with any portion of the socket. The resulting loads are calculated and assessed to the pre-determined limits of the hardware. Analysis results for Artemis II (and beyond) configurations showed that loads generated were well below the hardware limit, positive clearance was maintained between all other Core-SRB hardware, and no detrimental effects on the overall separation dynamics were observed.

Analysis of stressing vehicle configurations (primarily using ‘hottest’ or ‘coldest’ BSM propellant temperatures) showed that while the hottest BSM temperatures tended to increase the number of runs where this rubbing effect was observed, the magnitude of load experienced was comparatively the same (Figure 13). The addition of a custom contact model and loads metric to the existing booster separation analysis process provided a quantitative measurement to track this effect, and the decision was made to shorten the separation delay for Artemis II and beyond, realizing the desired vehicle performance gain.

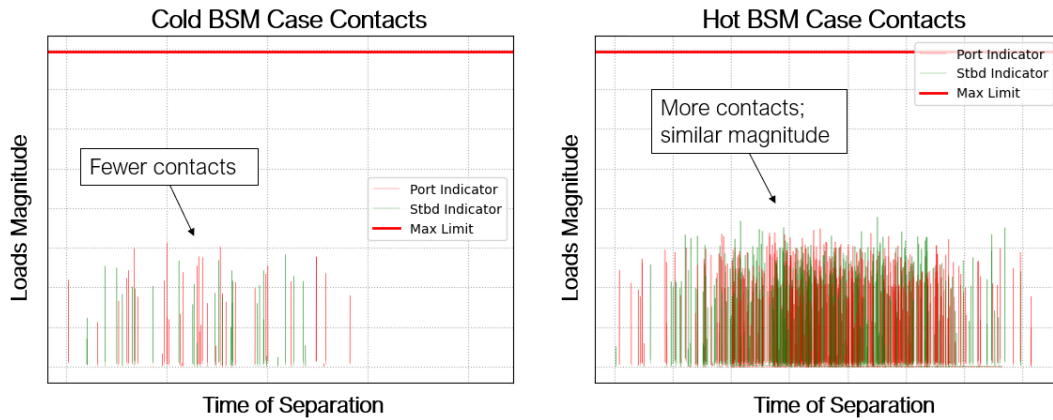


**Figure 13. Ball/Socket Contact Loads at Various Separation Times.** *Plot shows contacts for both left and right SRBs over two 2000-run Monte Carlo simulations.*

## POST-FLIGHT RESULTS

The November 16, 2022 Artemis I test flight provided the opportunity to validate simulation results with real-world test flight data. Since Artemis I was a night launch, this introduced several challenges for post-flight photogrammetry and trajectory reconstruction. Due to the dark lighting conditions and the plumes washing out the camera frames, only a qualitative comparison could be performed using the available imagery. Figure 14 shows a comparison of the simulated camera views and the actual in-flight camera imagery at selected frames during booster separation. The qualitative comparison shows very good agreement with the pre-flight simulation.

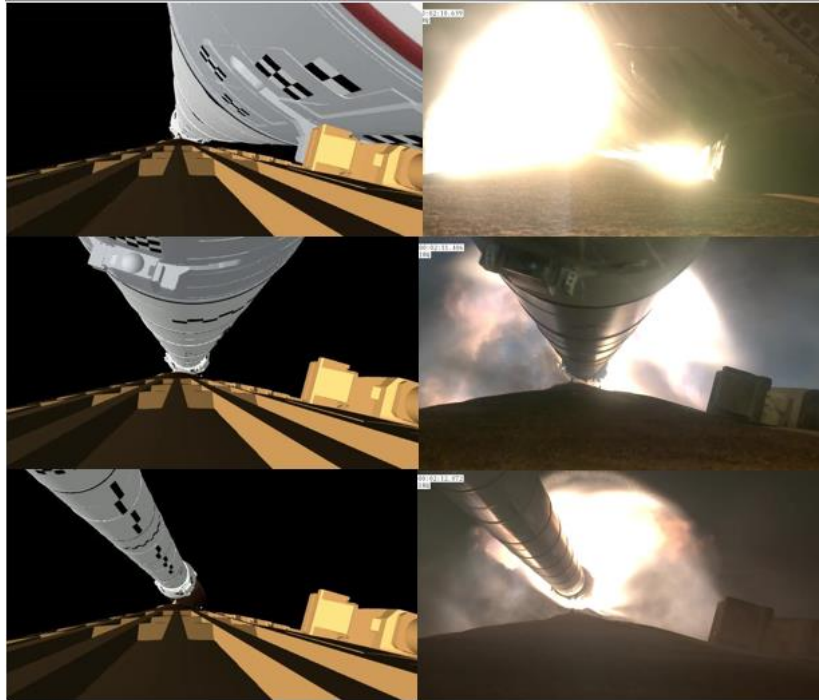


**Figure 14. On-Board Camera Views vs. Pre-Flight Predictions.** *Due to the night launch conditions and brightness of the SRB/BSM/RS-25 plumes, only a qualitative imagery assessment was performed, but good comparisons to pre-flight predictions were observed.*



A more quantitative comparison of predicted vs. actual separation clearances was still performed, using a version of CLVTOPS with the addition of post-flight reconstructed inputs for key models, such as CSE and SRB ignition times and engine performance, as-flown GN&C inputs, and day-of-flight mass properties. A single booster separation run was executed, and the results were compared to pre-flight predictions for three of the key clearances tracked for booster separation.

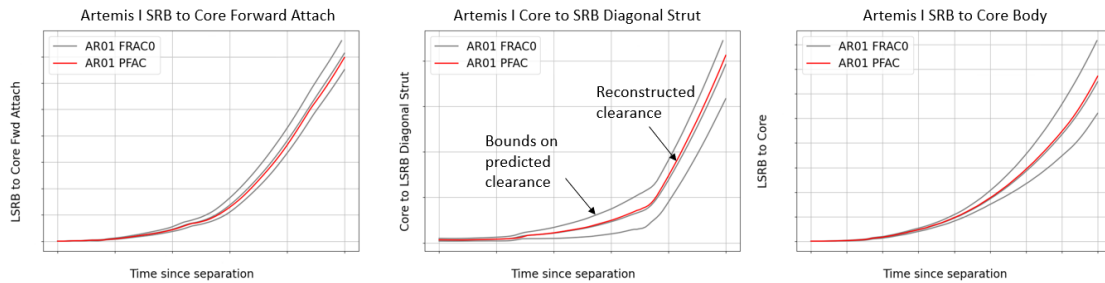


**Figure 15. Pre-Flight vs. Post-Flight Booster Separation Clearances.** *The reconstructed trajectory, using day-of-flight inputs and post-flight reconstructed inputs, showed excellent agreement with pre-flight predictions.*

The upper and lower gray lines in Figure 15 represent the 3-sigma high and low bounds on the pre-flight predicted clearance vs. time and were generated from a 2000-run Monte Carlo case. The middle gray line indicates the mean of these upper and lower bounds. The red line is the single reconstructed Artemis I booster separation trajectory from CLVTOPS, using the aforementioned day-of-flight inputs. The red line closely tracks the mean of the predicted performance envelope and does not exhibit any erratic or out-of-bounds behavior. In conjunction with the more qualitative assessment with the available imagery shown in Figure 14, these results give good confidence that the CLVTOPS simulation of the SLS booster separation event is a good representation of the actual Artemis I flight.

## CONCLUSION

Booster separation is a complex event that requires thorough analysis to ensure mission success and crew safety. The NASA MSFC-developed CLVTOPS toolchain provides a powerful suite of tools for simulation development, visualization, and post-processing, enabling the booster separation event to be studied with a high degree of fidelity and greatly increasing confidence of a successful flight. Input models are individually integrated and tested, which provides a thorough understanding of the effect of each one on the booster separation event and can sometimes lead to advantageous design changes or drive higher fidelity inputs. Monte Carlo studies are performed on a wide variety of vehicle configurations and separation conditions to ensure the chosen design and trajectory will result in success, within the defined requirements set out by the SLS program. Pre-flight predictions matched very well both qualitatively, with the available imagery, and quantitatively, using CLVTOPS with day-of-launch and reconstructed post-flight model inputs.

## REFERENCES

- <sup>1</sup> Orloff, Richard W., “Apollo by the Numbers: A Statistical Reference”, NASA History Division, Office of Policy and Plans, NASA SP-2000-4029, ISBN 0-16-050632-X, 2000.
- <sup>2</sup> Burger, Benjamin S.; Addona, Carole; Diedrich, Benjamin; Harlin, William J.; McDonough, Peter; Muscha, Zachary; Sells, Ray; and Tyler, Daniel, “Space Launch System Liftoff and Separation Dynamics Analysis Tool Chain”, *AIAA SciTech 2021 Forum*, DOI: 10.3514/6.2021-0822.
- <sup>3</sup> Schroeder, W., Martin, K., and Lorensen, B., “The Visualization Toolkit: An Object Oriented Approach to 3D Graphics”, 4<sup>th</sup> ed., Kitware, New York, 2006.
- <sup>4</sup> Elchert, K. C., “Space Shuttle Solid Rocket Booster Separation System”, Retrieved November 18, 2024 from <https://arc.aiaa.org/doi/pdf/10.2514/6.1982-1556>. DOI: 10.2514/6.1982-1556.
- <sup>5</sup> Tomlin, Donald D., “Space Shuttle Solid Rocket Booster (SRB) Separation”, NASA Technical Memorandum X-64967, November 1975. Retrieved from <https://ntrs.nasa.gov/api/citations/19760006102/downloads/19760006102.pdf> on December 12, 2024.
- <sup>6</sup> Lee, M., Dalle, D., Sanders, M., and Addona, C., “Development of Aerodynamic Loads Databases for the Space Launch System Booster Separation Event”, *AIAA SciTech 2024 Forum*, DOI: 10.2514/6.2024-0465.
- <sup>7</sup> McCarter, J. W., “Simulating Flights of Future Launch Vehicles and Spacecraft”, NASA Tech Briefs, 2007. Retrieved December 13, 2024 from <http://www.techbriefs.com/component/content/article/ntb/tech-briefs/software/1182>.
- <sup>8</sup> Hanson, J. M., and Beard, B. B., “Applying Monte Carlo Simulation to Launch Vehicle Design and Requirements Analysis”, Report Number NASA/TP-2010-216447.